Chapter

Analysis of Non-Rainfall Periods and Their Impacts on the Soil Water Regime

Milan Gomboš, Branislav Kandra, Andrej Tall and Dana Pavelková

Abstract

Rainfall and evaporation belong to the basic components of the hydrological cycle. Rainfalls are a decisive natural source of water in the soil. For water replenishment in the natural environment, it is important not only the sum of the rainfall for the balanced period but also the time distribution. In the case of long non-rainfall periods, the soil profile is dried. In the sufficiently long non-rainfall period, the water reserves in the unsaturated zone of the soil profile change and the actual evapotranspiration is reduced. There is a meteorological and then dry soil formation. For the design of adaptation measures, it is necessary to quantify the mentioned hydrological processes. These were investigated in the central area of the Eastern Slovak Lowland between 1970 and 2015. Significant non-rainfall periods, their periodicity and statistical characteristics have been identified. In the course of significant non-rainfall intervals during the vegetation periods the water reserves in the root layer of the soil were analysed up to a depth of 1 m, the actual and potential evapotranspiration, the evapotranspiration deficit, the groundwater level and the air temperature. The longest non-rainfall periods exceeded 30 days.

Keywords: rainfall, evaporation, non-rainfall periods, evapotranspiration deficit, soil drought

1. Introduction

Precipitation and evapotranspiration are basic compounds of hydrologic cycle. Precipitation is crucial natural source of water in the soil. Precipitation amount and temporal distribution of the rainfall is important for water refilling of the environment for balanced periods. Drying of soil profile occurs during long rainless periods. Meteorological drought and subsequently soil drought occurs in the case of the sufficiently long rainless period. Therefore it is necessary to know size and statistical characteristics of rainless periods (RLP).

For the analysis of the impacts of the length of the non-precipitation period on the soil water regime, it is necessary to analyse the second critical component of the hydrological cycle. It is a process of evaporation and quantification of the vapour. The evaporation of water in nature is physically the process of converting water to vapour. Due to the high vapour heat (2450 kJ kg^{-1} at the evaporating surface temperature of 20°C) it is an energy-intensive process. In nature, it is the decisive regulator of energy flows. The evaporation from the soil and plants is called evapotranspiration. The intensity of evapotranspiration over time is affected by the power consumption required for the phase conversion of water to vapour and the amount of this water in the environment. Consequently, evapotranspiration is seasonal in the course of the year. The decisive amount of water evaporates in the vegetal half of the year—from April to September. The maximum possible evapotranspiration under given meteorological conditions is potential evapotranspiration (ET_0). Its size is the result of the energy balance on the active surface. Really evaporated water from the soil and plants is called the actual evapotranspiration (ET_a). It depends on the positive energy balance, the turbulent exchange between the plant and the atmosphere, the water content of the soil profile, and the plant's ability to regulate the intake and discharge of water from its own organism. If there is sufficient water in the environment, then the actual evapotranspiration is the same as the potential evapotranspiration. If $ET_0 > ET_a$, there is an evapotranspiration deficit. This in the root zone of the soil profile indicates the water supply deficit and the beginning of the soil profile drying. Current climate changes are reflected in the redistribution of precipitation over the course of the year and the increase in the air temperature. In other words, the distribution of water and energy in the hydrological system is redistributed. These changes are reflected in changes in evaporation and consequently in changes in the water balance of the area [1–6]. The authors of the chapter have the hypothesis that not only the height of precipitation but also their time distribution during the year has the effect on the occurrence of soil drought.

The aim of the chapter is to identify significant non-precipitation periods, to quantify their time duration, probability properties, development trends and impacts on changes in the critical components of the water regime in the soil environment. In the course of significant non-precipitation intervals during vegetation periods, the water reserves in the root layer of the soil up to a depth of 1 m, the actual and potential evapotranspiration, the evapotranspiration deficit, the groundwater level and the air temperature were analysed.

2. Materials and methods

The identification of non-precipitation periods and the process of their impact on the components of the water regime of the soil environment were examined in the Milhostov locality in the Eastern Slovak Lowlands (ESL).

The analysis concerned the growing seasons from 1970 to 2015. During the analysis, the following values were analysed at 1-day calculation step and one-day input data: non-rainfall periods, soil water storage to the depth of 1 m; movement of the groundwater level; air temperature; and daily totals of actual and potential evapotranspiration, rainfall and evapotranspiration deficiency.

The research was based on field measurements of hydrophysical characteristics, volume humidity monitoring over the soil profile vertical line, laboratory work and numerical simulation of the water regime using GLOBAL mathematical model [1–6]. The part of the research works was also the verification of the mathematical model using results of the monitoring carried out in the examined locality.

2.1 Description of the investigated area

These hydrological processes were examined in Milhostov, the area located in the central part of the ESL, Slovakia (48°40′11.08″, N; 21°44′18.02″, E; 100 m). The selected area is characteristic of the ESL. Typical soil of the area is gleyic fluvisol, a medium-heavy soil where clay particles forms 11–39% of the content.

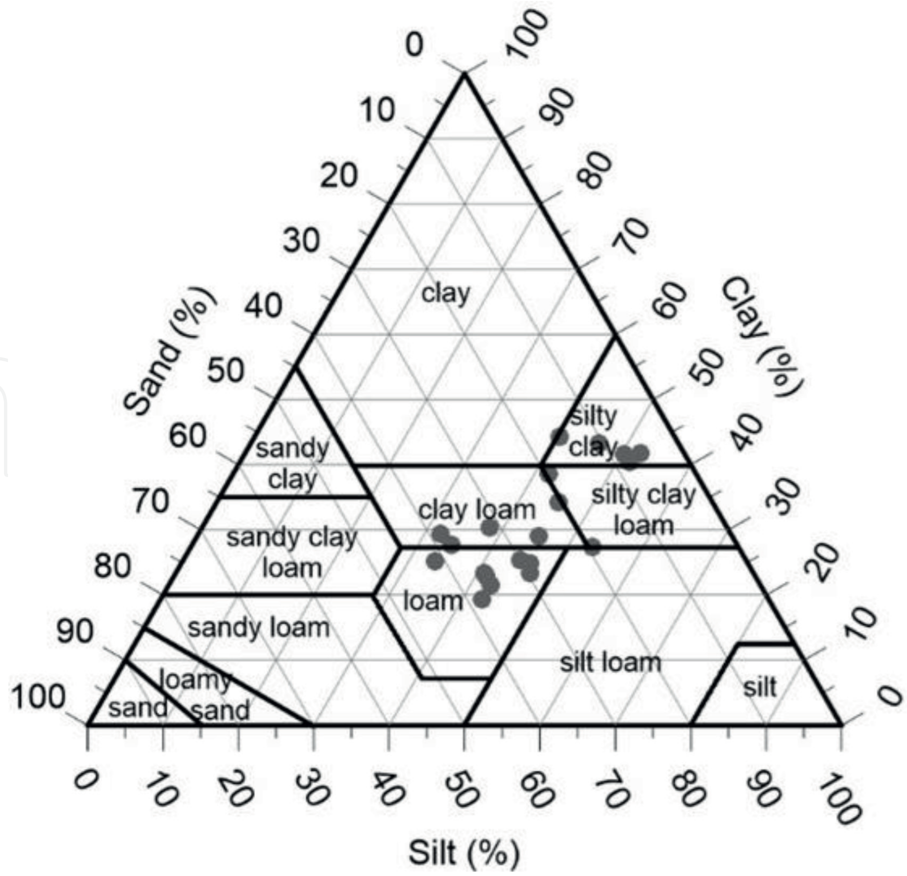

Figure 1.
Texture of the examined soil profile as defined by the USDA triangle (sand 0.05–2.0 mm, clay <0.002 mm, silt 0.002–0.05 mm).

The profile is made of clay, clay-loam and silty clay layers **Figure 1**.

Figure 2 shows the course of the clay, dust and sand content via the vertical line of the soil profile by 0.1 m layers to a depth of 1.0 m.

The clay, silt and sand content via the vertical line of the soil profile to 1 m depth. **Figure 2** shows that the most ratio of the studied profile is formed by the dusty component. The profile is up to 0.7 m relatively homogeneous. In the range between 0.7 and 1.0 m, the ratio of the individual components of the microstructure significantly changes. For this reason, two material layers were considered in the calculations. **Table 1** lists their retention lines parameters according to Van Genuchten.

In terms of climate, the examined area, as well as the rest of the ESL, is located in the transitional climate region between the maritime and the continental climate. In terms of temperature, the area is homogeneous. Long-term mean temperature in the area between the years 1961 and 2015 is 9.4°C; minimum mean daily temperature is −20.5°C, maximum mean daily temperature is +30.6°C. The absolute minimum temperature in the area during the analysed period was −29.1°C (January 01, 1987) and the absolute maximum daily temperature was +38.2°C (July 22, 2007). The warmest month is July, the coldest is January. The mean annual amount of rainfall in the area is 558 mm (years 1961–2015). Daily maximum rainfall total was 82.5 mm (June 26, 1995). Rainfall conditions in the area are heavily influenced by the air circulation. Heaviest rainfall is induced by the humid and warm air flowing from the south. Air currents from the other directions do not usually bring rainfall because it falls on the Carpathians. The maximum duration of the continuous period with no rainfall was 35 days. The maximum annual long-term mean duration of the period with no rainfall is 17 days. Long-term mean

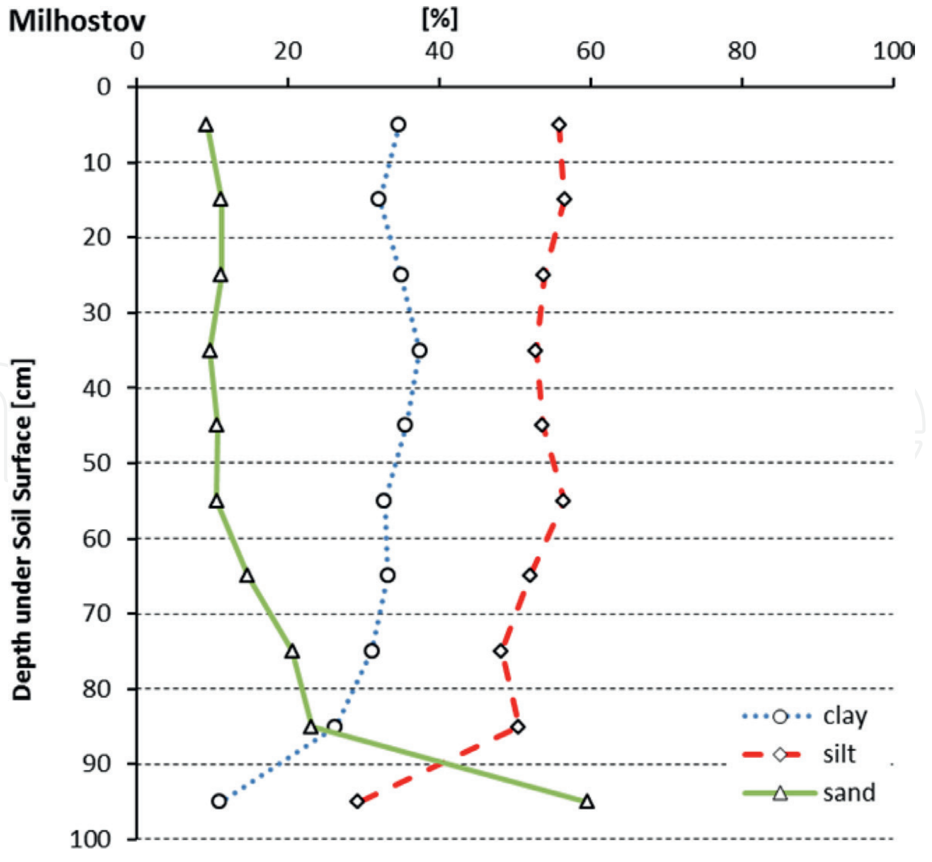

Figure 2.
Content of clay, silt and sand to the soil profile vertical to 1 m depth.

Layer	Alpha	n	θs	Θ_r
0.0–0.7 m	0.0084	1.5202	0.43	0.12
0.7–1.0 m	0.0482	1.1593	0.39	0.07

Table 1.
Parameters of retention lines of material layers of the soil profile.

wind speed 10 m above the ground is 2.468 m s^{-1}. Daily long-term mean pressure of water vapour is 0.999 kPa where the daily mean minimum is 0.083 kPa and the maximum is 2.760 kPa. Daily long-term mean relative humidity is 77.4%, where the daily mean minimum is 33% and the maximum is 100%. With regard to phenological characteristics and vegetation of the area, there are no noticeable temporal or local changes.

2.2 Description of the experiment

Methodical process of the research consists of two phases: rainless periods selection, model verification, calculation of water regime components and results interpretation. Climatic station of Milhostov (N 48°39,786′; E 21°43,298′) was chosen for selection of statistically important rainless periods. Station is located at central part of Eastern Slovak Lowland (ESL) and represents wider area of lowland. Daily precipitation amounts of the 1961–2015 period was examined for the station. 20,080 daily precipitation amounts (including zero) were analysed for the period. Length of RLP was identified separately for whole years of examined periods and separately for vegetal periods (VP). Selections of RLP were applied for VP examination in two ways. Periods with zero daily precipitation amounts were considered in first selection (s0). Daily precipitation amounts lower than 2 mm were considered as zero in the second selection (s2). These precipitation are likely to be catched by the plant cover and subsequently vaporised without influencing soil water supply. Selection of rainless periods during VP was done only of those which occurred during vegetal periods (April–September). However, periods that starts before VP and overlap to VP and those that starts during VP and finished after VP were considered as well. Rainless periods of the 1961–2015 were probability-evaluated in every selection group.

Just (s0) selection was applied during examination of entire year periods. Basic statistical characteristics were calculated after identification of RLP. Probability characteristics of occurrence of different RLP temporal duration were calculated by binomial distribution. The results are indicated in the form of frequency curves. Development of number of rainless days during individual years and VP was evaluated. For example, 10 longest RLP during 1961–2015 were selected for every selection.

The database for needs of the experiment was collected by the field monitoring, laboratory measurements and the numerical simulation via the mathematical model 'GLOBAL'.

The field monitoring concerned the measuring of the groundwater level and volumetric moisture within a soil profile, vertically to the depth of 0.8 m and horizontally by 0.1 m thick layers. The field works included also soil sampling. Gathered soil samples were processed in the laboratory and basic characteristics of the soil profile were determined. The Climatic and Agroecology Research Institute is located in the examined area. During the years 1970–2015, the institute provided hydro-meteorological data and plant characteristics necessary for the numerical simulation via the mathematical model 'GLOBAL'. The results of the water storage monitoring to the depth of 0.8 m are available as well. The model was verified using the data from the extremely dry growing season in 2007. The growing season of 2007 was the second driest season of the analysed period. The driest season was that of the year 2015.

Once the model was verified, the development of ET_0, ET_a and water storage in a soil profile to the depth of 1 m was calculated with one-day calculation step. In addition, the value of evapotranspiration deficiency was calculated using Eq. (1):

$$D = ET_0 - ET_a \tag{1}$$

The simulation was conducted for the growing seasons from 1970 to 2015. ET_0, ET_a and D totals during the growing seasons were analysed with regard to water storage (WS), rainfall and groundwater level (GWL). For ET_0, ET_a and D, linear trends were calculated and the correlation analysis between the analysed units was performed. The development of WS in the extremely dry season was analysed with one-day step.

2.3 Brief description of the model 'GLOBAL'

The model 'GLOBAL' is a mathematical model to enable simulating water movement in soil and calculating the distribution of soil moisture potential, i.e. soil moisture in real time [7–12]. The model is based on the numerical solution of a non-linear partial differential Richards' equation describing water movement in aerated soil zone, which is as follows:

$$\frac{\partial h_w}{\partial t} = \frac{1}{c(h_w)} \frac{\partial}{\partial z} \left[k(h) \left(\frac{\partial h_w}{\partial z} + 1 \right) \right] - \frac{S(z,t)}{c(h_w)} \tag{2}$$

where h_w—soil moisture potential; z—vertical coordinate; $k(h_w)$—unsaturated hydraulic conductivity of soil; $S(z,t)$—intensity of water uptake by plant roots from unit soil volume per unit of time (cm^3/cm^3).d^{-1}; and $c(h_w) = \frac{\partial\theta}{\partial h_w}$, θ—volume soil moisture (cm^3/cm^3).

The simulation using the model 'GLOBAL' can be performed with one-day calculation step. In that instance, daily values are used as the input values for creating the boundary conditions. This also applies to the meteorological inputs and the plant cover input parameters. The model 'GLOBAL' includes also soil hydrophysical characteristics such as: retention curves, soil saturated and unsaturated hydraulic conductivity, hydrolimits and some physical soil characteristics (porosity, specific weight and volumetric mass density and moisture of saturated soil). In the model, hydrophysical characteristics are expressed by analytical equations. Moisture retention curve is described by van Genuchten model.

Potential evapotranspiration ET_0 is calculated by Penman-Monteith equation. For determining actual transpiration and evaporation, the method developed at IH SAS was used. This method assumes that the evapotranspiration depends on the value of leaf area index (LAI). The intensity of potential evaporation E_{eo} is calculated from the value of potential evapotranspiration ET_0 as follows:

$$E_{eo} = ET_0 . \exp(-m_1 . LAI) \quad (3)$$

The value of empirical coefficient (m_1 = 0.463) was gained by field measurements in a maize field. Actual evapotranspiration and its structure is calculated based on the values of potential evapotranspiration ET_0 and the relation between relative evapotranspiration E_{eo}/ET_0 and soil profile moisture, i.e.

$$ET_r = \frac{E_{eo}}{ET_0} = f(\theta) \quad (4)$$

The calculation method is based, inter alia, on the assumption that the median soil moisture in the root zone used for the calculation of transpiration, or the value of moisture in the upper layer of a soil profile used for the calculation of evaporation, depends on the intensity of evaporation. The higher is the intensity of evaporation, the higher is the value of θ_k, at which the evaporation starts to decrease. The verification of the method via the model 'GLOBAL' has shown a very high concordance between the calculated values and the values measured in real conditions. The outputs of the modelling are moisture and soil moisture potential distribution, daily totals of the following: interception, evaporation and its components, infiltration, existing water deficiency in soil and other.

3. Results and discussion

3.1 Identification of non-precipitation periods

Basic characteristics of descriptive statistics are indicated in **Table 2**. It results that 12,185 days (60.68%) were with no precipitation in 1 year selection data series. Days without rainfall were grouped to 3409 periods. 63.87% of days without rainfall were in the case of VP and s0 selection and 85.12% days without rainfall in the case of VP and s2 selection. The longest RLP duration was 35 days for s0 selection and 53 days for s2 selection.

Eloquent image of probability of occurrence of maximal year durations of RLP gives probability of exceedance curves. Curves are indicated in **Figure 3**. There of

Parameters	Year	VP	VP
Selection	f(0)	f(0)	f(2)
Mean	3.57	3.67	6.15
Standard error	0.06	0.08	0.17
Median	2	2	4
Mode	1	1	1
Standard deviation	3.52	3.51	6.31
Sample variance	12.41	12.30	39.84
Kurtosis	10.98	9.66	8.47
Skewness	2.64	2.47	2.45
Range	34	34	52
Minimum	1	1	1
Maximum	35	35	53
Sum	12,185	6429	8567
Count	3409	1751	1393
Confidence level (95.0%)	0.12	0.16	0.33

Table 2.
Basic statistical characteristics of rainless periods.

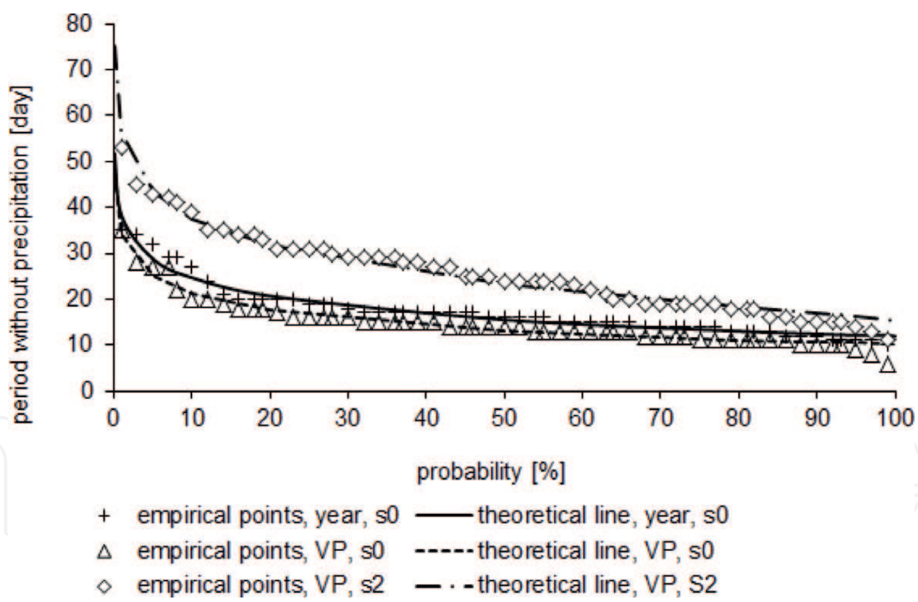

Figure 3.
Empirical and theoretical probability of exceedance curves of maximal year durations of rainless periods.

results that only little differences are between course of yearly and vegetal selections of s0. Length of RLP with p = 50% probability of exceedance is for this selection of VP 13 days and for the year 15.5 days. This value is 23.3 days for selection s2 during the vegetal period. The course of probability of exceedance curve is in case of s2 selection moved and more steep. This indicates greater variability and longer duration of RLP.

Numbers of days without rainfall are indicated in **Figure 4** for individual years and their vegetal periods for selections s0 and s2. Developmental trends are for all cases parallel with timeline. It is testified by the fact that number of rainy

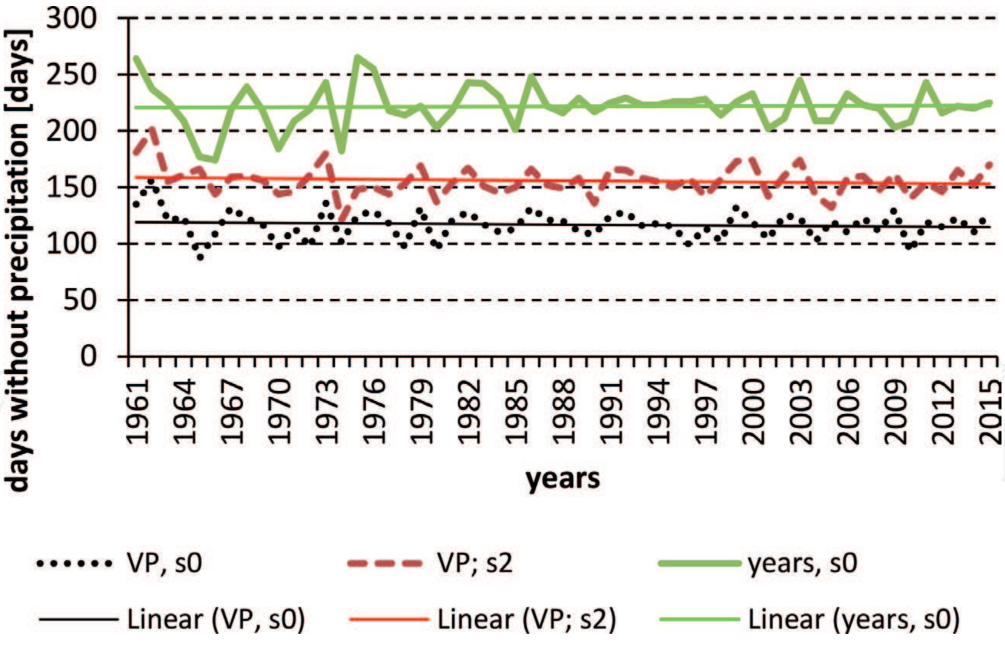

Figure 4.
Number of days without precipitation in individual years 1961–2015.

and rainless days is for individual years and their vegetal periods balanced in the long term view. Only duration of rainless events of non-vegetal periods changes in examined periods. It is confirmed by the results that are graphically shown in **Figure 5**. There are indicated numbers of days of rainless periods that lasts 10 days or more for VP of individual years. From the figure results that trend development of both selections s0 and s2 is stable without change (parallel to the timeline) during vegetal periods. Elongated trend of rainless periods with duration of 9 days or more was identified in case of s0 yearly selection. These results show that this trend

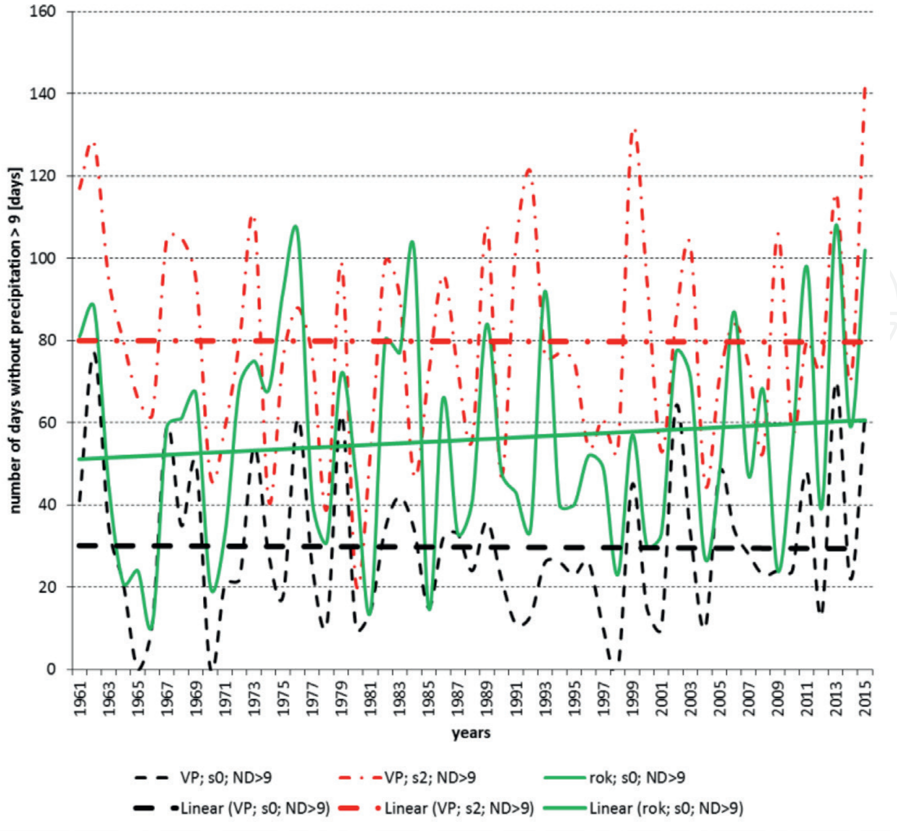

Figure 5.
Number of days during rainless periods with duration of 9 days or more.

DOI: http://dx.doi.org/10.5772/intechopen.82399

is caused by rainless events during non-vegetal periods. Stated fact has influence on creation of water storage during before-spring periods and enlarges risk of drought.

As an example, 10 longest rainless periods with date of its occurrence, theoretical probability and periodicity of incidence is indicated in **Table 3** for every selection series (year, s0, VP, s0 and VP, s2). The absolutely longest continuous period without rainfall for s0 selection (year, VP) had 35 days and occurred between 25.9.1962 and 29.10.1962. Maximal continuous rainless event extends to 53 days in case of s2 selection for the vegetal period. This event occurred in time interval 19.7.1967–9.9.1967. Precipitation amount was only 1.6 mm in this time interval. This time interval can be considered as the rainless period. From **Table 3** results that the most important rainless periods predominantly occurred in 1960s and after the year 2000.

Extremely dry year 2015 does not appear in s0 selection, however, it was identified in s2 selection. 35 day continuous period during which was total precipitation amount of 2.5 mm occurred. This year was unique in that 91 rainless days between 28.5.2015 and 2.9.2015 were associated in 4 seasons by 18, 22, 16 and 35 days in selection s2.

3.2 Model verification

During the verification of the model GLOBAL the assessment of the weekly values of integral soil water content to the depth of 0.8 m expressed in millimetres of water column was conducted. The selection of the layer for the calculation

Daily precipitation totals to 0,0 mm; period year					Daily precipitation totals to 0,0 mm; vegetation period					Daily precipitation totals to 2,0 mm; vegetation period				
start PWP	end PWP	number	theoretical value		start PWP	end PWP	number	theoretical value		start PWP	end PWP	number	theoretical value	
from	to	of days	probability	periodicity	from	to	of days	probability	periodicity	from	to	of days	probability	periodicity
date		[days]	[%]	[years]	date		[days]	[%]	[years]	date		[days]	[%]	[years]
25.09.62	29.10.62	35	1,0	105	25.09.62	29.10.62	35	2,3	43	19.07.67	09.09.67	53	2,1	48
22.10.11	24.11.11	34	1,1	87	18.03.74	14.04.74	28	6,0	17	09.09.06	23.10.06	45	4,5	22
30.01.76	01.03.76	32	2,0	49	05.08.76	31.08.76	27	7,2	14	19.09.62	31.10.62	43	5,4	18
16.02.74	16.03.74	29	3,3	30	14.03.05	09.04.05	27	7,2	14	08.09.61	19.10.61	42	6,3	16
22.10.75	19.11.75	29	3,3	30	15.09.11	06.10.11	22	16,8	6	12.08.74	21.09.74	41	7,1	14
18.03.74	14.04.74	28	3,8	26	24.03.99	12.04.99	20	24,2	4	23.09.00	31.10.00	39	8,8	11
05.08.76	31.08.76	27	4,2	24	23.03.02	11.04.02	20	24,2	4	06.04.62	10.05.62	35	14,3	7
14.03.05	09.04.05	27	4,2	24	02.07.06	20.07.06	19	30,0	3	05.09.89	09.10.89	35	14,3	7
05.10.65	28.10.65	24	6,6	15	14.09.75	01.10.75	18	35,8	3	30.07.15	02.09.15	35	14,3	7
15.09.11	06.10.11	22	9,2	11	17.06.76	04.07.76	18	35,8	3	16.05.64	18.06.64	34	16,0	6

Table 3.
Ten longest rainless periods in every selection series, their theoretical probability of incidence and periodicity.

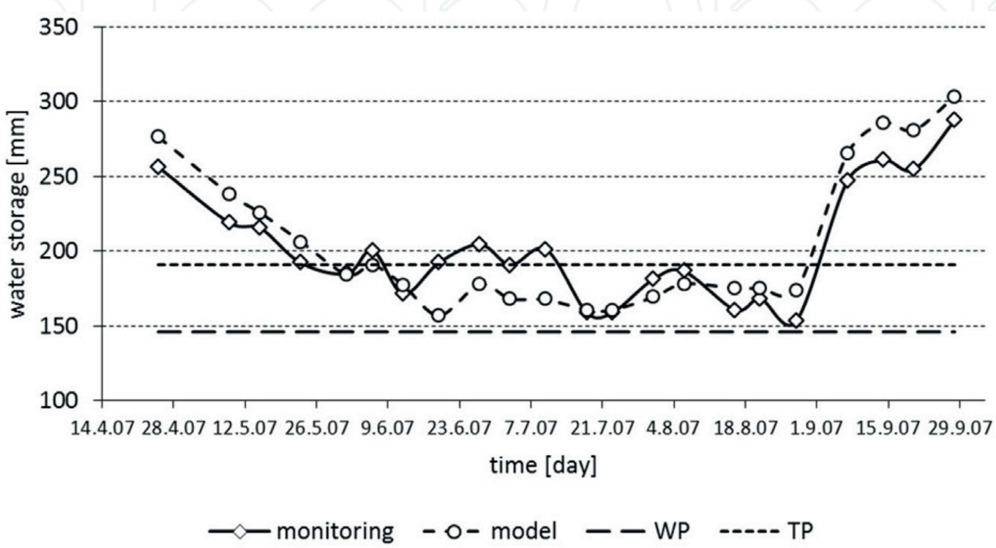

Figure 6.
Comparison between the monitored and the modelled soil water storage up to the depth of 0.80 m during the growing season of 2007.

depended on the depth to which the soil water storage was monitored in field. The results of the simulation and the measurements are shown in **Figure 6**. The diagram shows a very high concordance between the calculated and the measured values which is proven by the results in **Figure 7**. It is a quantile-quantile plot which shows the linear trend and the correlation coefficient between the measured and the modelled values. The R-squared statistic indicates that the model as fitted explains 86.37% of the variability in measurement. The correlation coefficient equals 0.93, indicating a relatively strong relationship between the variables. Other basic characteristics of the descriptive statistics are listed in **Table 4**.

The results show that, especially in terms of moisture, the model GLOBAL $\theta > TP$ tends to overestimate the real state. When the moisture is lower, it tends to underestimate it. In addition, the t-test was applied to compare the mean values and the F-test to compare the standard deviations of the measured and the modelled values. The results of the tests are shown in **Table 5**. The tests showed that the null hypothesis regarding the equality of the mean values and standard deviations of

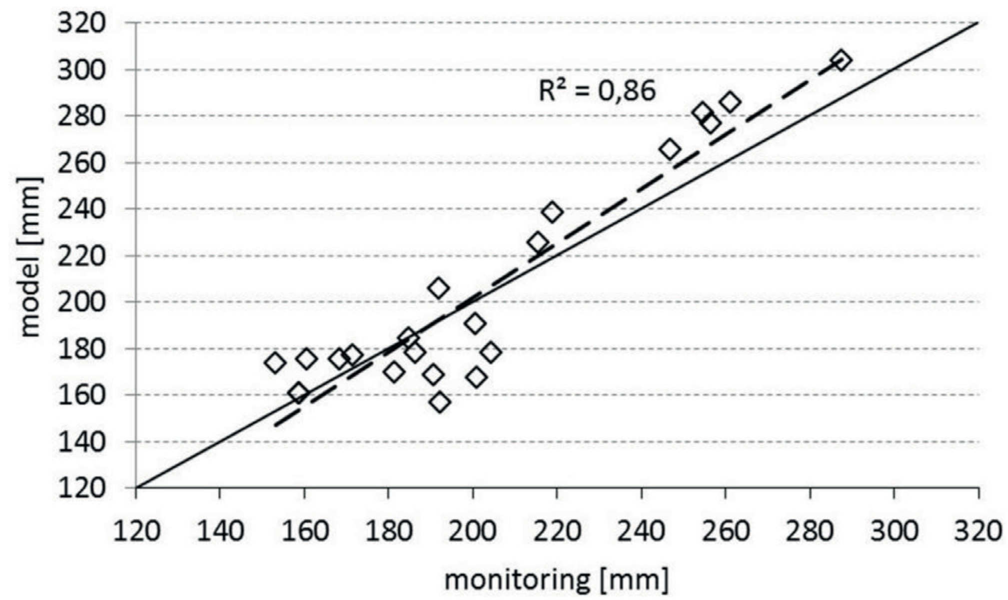

Figure 7.
Representation of the linear dependence via the correlation coefficients between the measured and the modelled daily values of integral soil water content to the depth of 0.8 m in Milhostov.

Statistics	Measurement	Simulation
Count	22	22
Average	202.12	204.43
Standard deviation	37.89	47.84
Variance	1435.57	2288.79
Coefficient of variation	18.75%	23.40%
Minimum	153.32	157.09
Maximum	287.38	303.43
Range	134.07	146.34
Standard skewness	1.455	1.877
Standard kurtosis	−0.284	−0.584

Table 4.
Summary statistics.

t-Test to compare means	
Null hypothesis	Mean measurement = Mean simulation
Alternative hypothesis	Mean measurement ≠ Mean simulation
t-statistic = −0.177316	Two-sided P-value = 0.860112
Conclusion	Do not reject the null hypothesis for alpha = 0.05
F-test to compare standard deviations	
Null hypothesis	Sigma measurement = Sigma simulation
Alternative hypothesis	Sigma measurement ≠ Sigma simulation
F-statistic = 0.627217	Two-sided P-value = 0.293035
Conclusion	Do not reject the null hypothesis for alpha = 0.05

Table 5.
Results of the t-test and F-test.

the measured and simulated values cannot be rejected. The results indicate that the model is suitable for the examined area and it can be used for the simulation of the water regime in the unsaturated soil zone. It should be noted that the model has been verified and successfully applied in other areas around Slovakia (Novák et al., 1998).

Figure 8 shows the contour lines representing the volume moisture and it was made based on the moisture values monitored up to the depth of 0.8 m by 0.10 m thick layers in Milhostov during the growing season of 2007. The picture shows that the whole profile was dry to the subsoil layers.

3.3 Results of numerical simulation

Table 6 lists the basic characteristics of the descriptive statistics applied to the following: seasonal, monthly and daily totals of ET_0, D, P; average soil water storage during the growing season to the depth of 1.0 m and the mean location of GWL under the surface during the growing season. **Table 6** shows that the long-term mean evaporation during the growing season in the form of ET_a is 315.17 mm (59.4% of ET_0) while evaporation ET_0 is 530.63 mm. This leads to the long-term evaporation deficiency of 215.45 mm, which is 40.6% of ET_0. Long-term mean rainfall total during the growing season is 70.0% (371.44 mm) of ET_0. Long-term mean

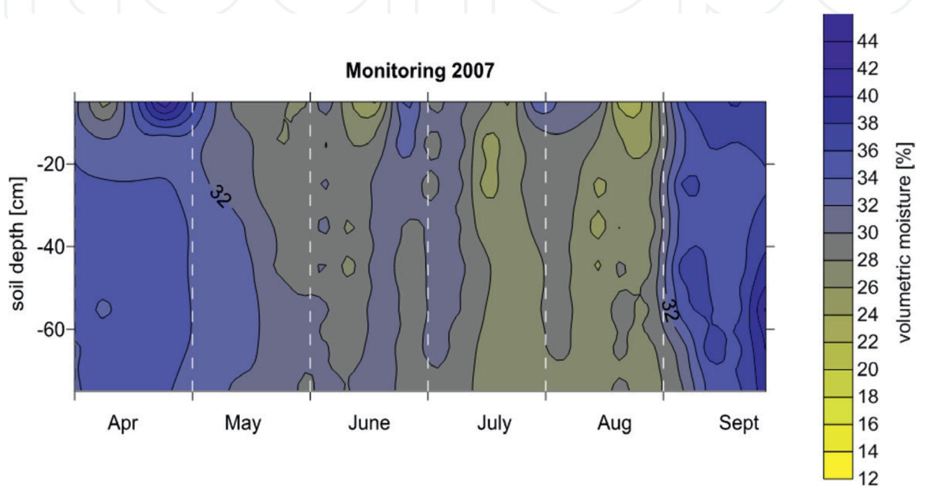

Figure 8.
Contour lines of the volumetric moisture up to 0.80 m during the growing season of 2007.

Statistic	VO						Month		Day	
	ET_0	ET_a	D	WS	P	GWL	ET_0	ET_a	ET_0	ET_a
	[mm]					[cm]	[mm]		[mm]	
Mean	530.6	315.2	215.5	278.4	371.4	135.1	88.4	52.5	2.9	1.7
St. er.	12.0	11.7	16.1	5.5	12.7	3.6	1.5	1.3	0.0	0.0
Median	533.5	290.7	209.0	270.2	360.9	136.2	87.3	51.1	2.8	1.6
St. dev.	81.1	79.5	109.4	37.2	85.9	24.1	25.1	21.9	1.4	1.1
S. var.	6580.3	6316.8	11958.3	1384.9	7373.9	580.3	631.8	477.5	1.9	1.1
Kurtosis	0.5	0.1	1.3	1.2	2.03	3.8	−0.3	0.5	0.1	0.3
Skew.	−0.2	0.7	0.8	0.9	0.93	0.2	0.3	0.5	0.3	0.6
Range	409.9	370.2	556.4	187.0	444.4	159.6	131.9	121.3	9.3	6.0
Min	302.7	156.1	0.2	213.6	226.8	61.1	28.3	3.3	0.0	0.0
Max	712.6	526.2	556.6	400.6	671.2	220.7	160.2	124.5	9.3	6.0
Count	46	46	46	46	46	46	282	282	8235	8235

Table 6.
Statistical characteristics of the seasonal, monthly and daily totals of ET_o, ET_a, D, WS, P and GWL.

monthly total of ET_a is 88.44 mm. Long-term mean daily total of ET_a is 1.73 mm while ET_0 is 2.91 mm. Mean depth of the GWL under the surface is 135.09 cm. **Table 6** shows statistical characteristics of the seasonal, monthly and daily totals of ET_0, ET_a, D, P; mean soil water storage during the growing season to the depth of 1.0 m and mean location of the GWL under the surface during the growing season.

Figure 9 shows the long-term mean values of the monthly total of ET_0, ET_a and D. The results indicate that the highest long-term mean monthly total of evaporation deficiency is in July and August. It is caused by the fact that the mean monthly soil water storage gradually diminishes during the growing season until July when it stops at the minimum value. To the contrary, ET_a increases and reaches the top value in July. The maximum value of long-term mean total of ET_a occurs in June when soil profile contains enough water. From June until the end of the growing season ET_a continuously drops.

Figure 10 shows the development of D, ET_0, ET_a, P totals, mean soil water storage to the depth of 1 m (WS), mean temperatures (T) and mean GWL during the growing seasons between 1970 and 2015.

It is obvious that during the examined period, the difference between ET_0 and ET_a raised. Evaporation deficiency 'D' therefore increases. Variability has also grown during the last 15 years. As for standard deviation 'D', from 1970 to 1985 it was 63 mm, from 1986 to 2000 it was 69 mm and during 2001–2015 it reached 158 mm. The variability has raised in all examined parameters during the last 15 years (e.g. WS raised by 50%). With the exception of evaporation, the trends are balanced.

Table 7 correlates the examined parameters. The most significant and closest relation is between soil water storage and D (**Figure 11**) and GWL which are inversely proportional. On the other hand, water storage in the root zone of a soil profile statistically depends on GWL and ET_a.

The processes can be explained by the fact that GWL is a lower boundary of the unsaturated soil zone and for the purpose of soil water regime, it is defined as the lower boundary condition. The lower boundary of the unsaturated soil zone is thus dynamic and, depending on the interaction with the groundwater, it can change in space and time. When GWL is high, groundwater can reach the soil profile. In depressed lowland areas, such as ESL, groundwater often reaches the surface of the ground and the unsaturated soil zone is lost. Due to its fluctuation

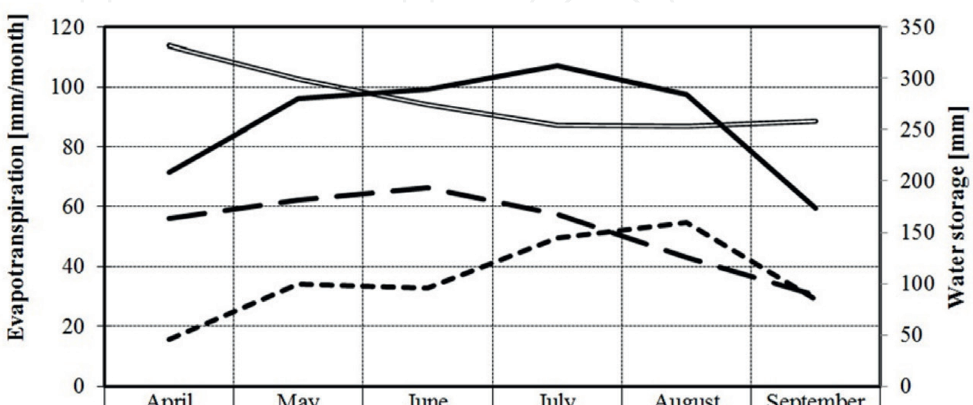

	April	May	June	July	August	September
ET0	71	96	99	107	98	59
ETa	56	62	66	58	43	30
D	16	34	33	49	55	29
WS	332	299	275	254	253	258

Time [month]

Figure 9.
Long-term mean monthly totals of ET_0, ET_a and D.

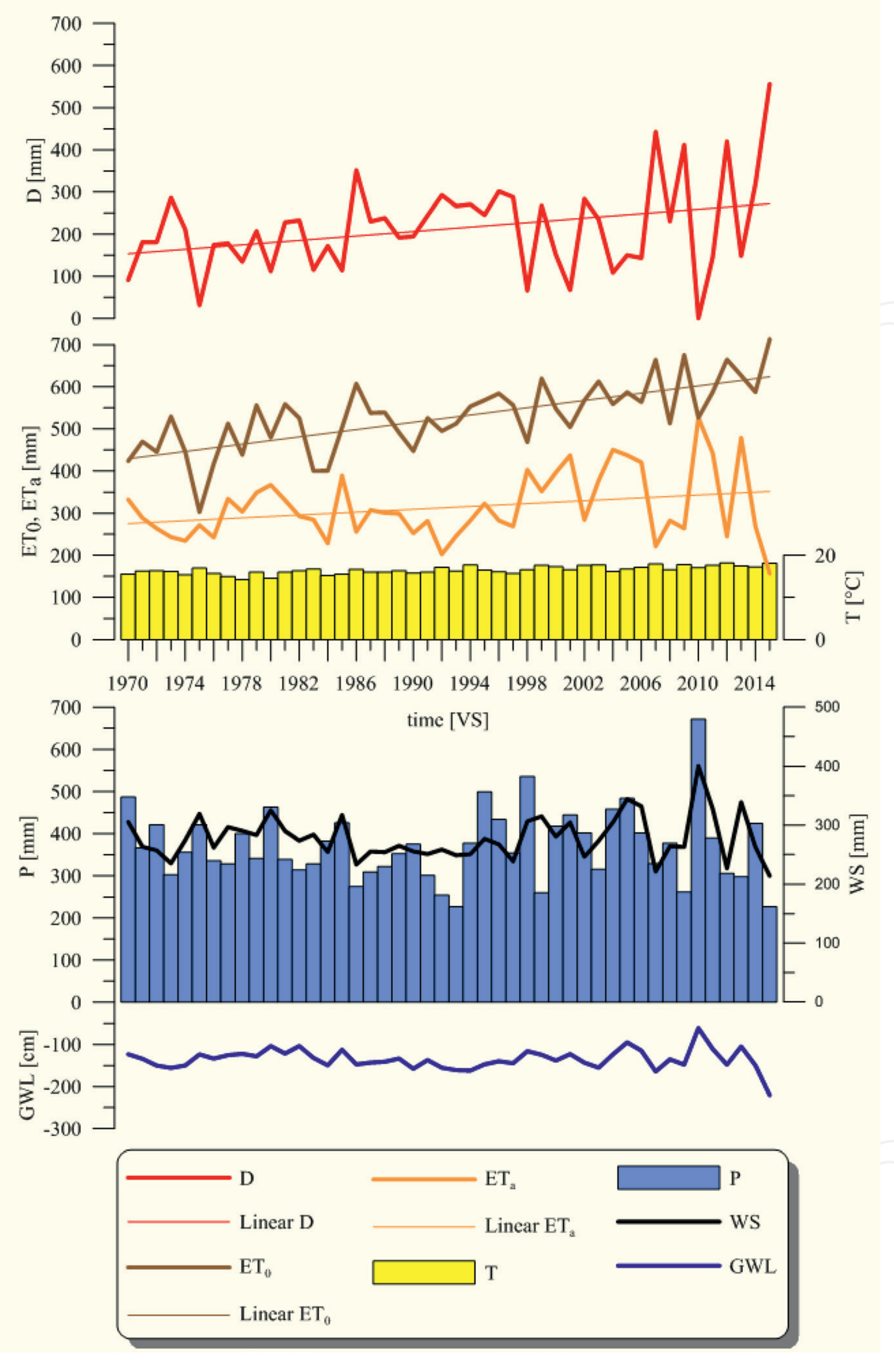

Figure 10.
Evapotranspiration deficiency and the water regime elements during the growing seasons 1970–2015.

in time, groundwater can reach the soil profile even when the average GWL is lower. In this way, the interaction processes influence on the soil water storage and its availability for the plant cover. It is especially observable during periods of meteorological drought. During longer periods with no rainfall, precipitation cannot cover the actual evapotranspiration ET_a and the drying process begins. There is a slight retardation in time in terms of the impact of the drying process on GWL and the unsaturated soil zone. In lowland areas, first layers to be dried are the upper layers of a soil profile. Drying then spreads to the lower layers towards GWL. Time retardation lies in that groundwater supplies the

Parameters	P [mm]	ET_0 [mm]	ET_a [mm]	T [°C]	GWL [cm]	WS [mm]	D [mm]
P [mm]	1.0						
ET_0 [mm]	−0.3	1.0					
ET_a [mm]	0.6	0.1	1.0				
T [°C]	−0.2	0.6	0.0	1.0			
GWL [cm]	0.6	−0.3	0.8	−0.2	1.0		
WS [mm]	0.6	−0.2	0.9	−0.1	0.9	1.0	
D [mm]	−0.7	0.7	−0.7	0.4	−0.8	−0.8	1.0

P—precipitation, ET_0—potential evapotranspiration, ET_a—actual evapotranspiration deficiency, T—mean temperatures, GWL—groundwater level, WS—water storage, D—evaporation.

Table 7.
Correlation table of the examined parameters.

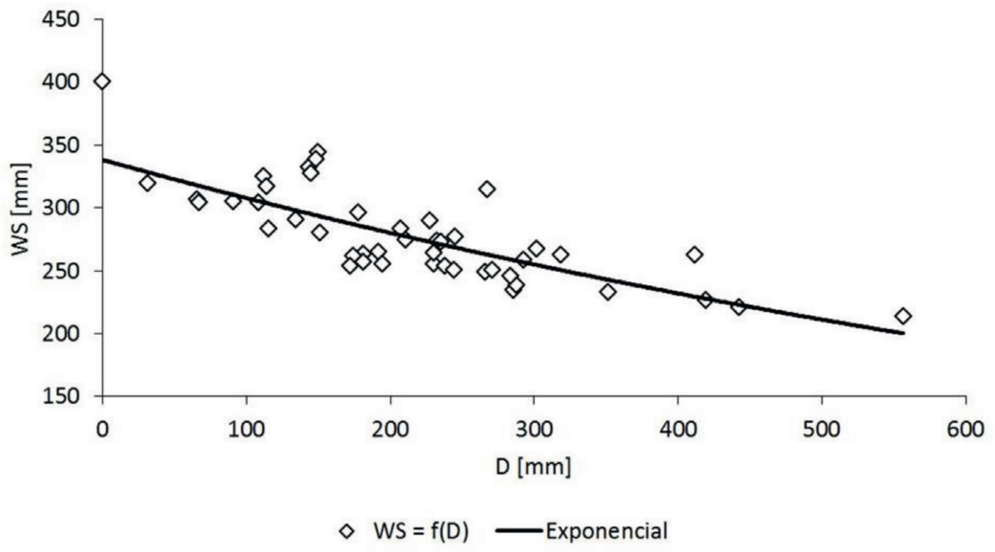

Figure 11.
Graphical representation of the exponential dependence between evapotranspiration deficiency (D) and water storage (WS) in soil to the depth of 1 m; R = 0.8.

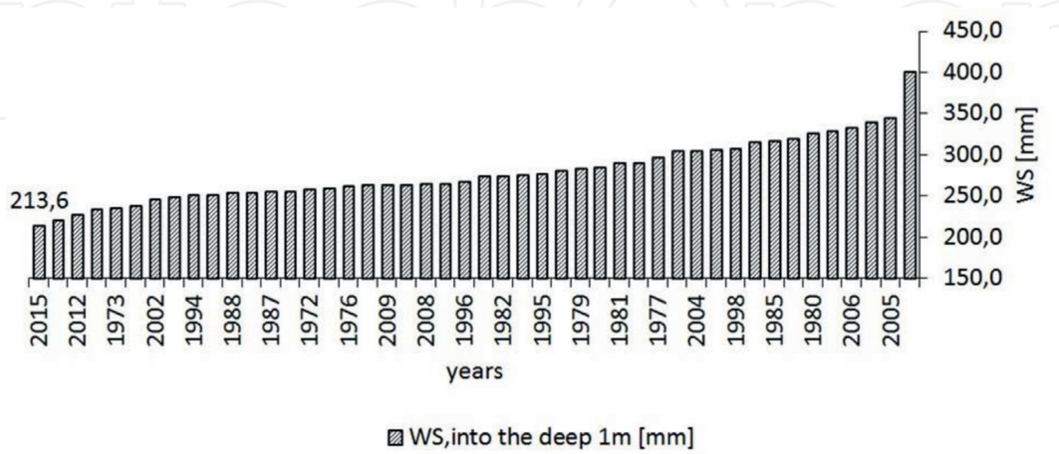

Figure 12.
Growing seasons 1970–2015 ordered by soil water storage in a soil profile to the depth of 1 m.

unsaturated soil zone with water and thus ameliorates its availability for the root zone of the plant cover. In consequence, GWL drops and the unsaturated soil zone becomes thicker. When GWL drops under the critical (threshold) point,

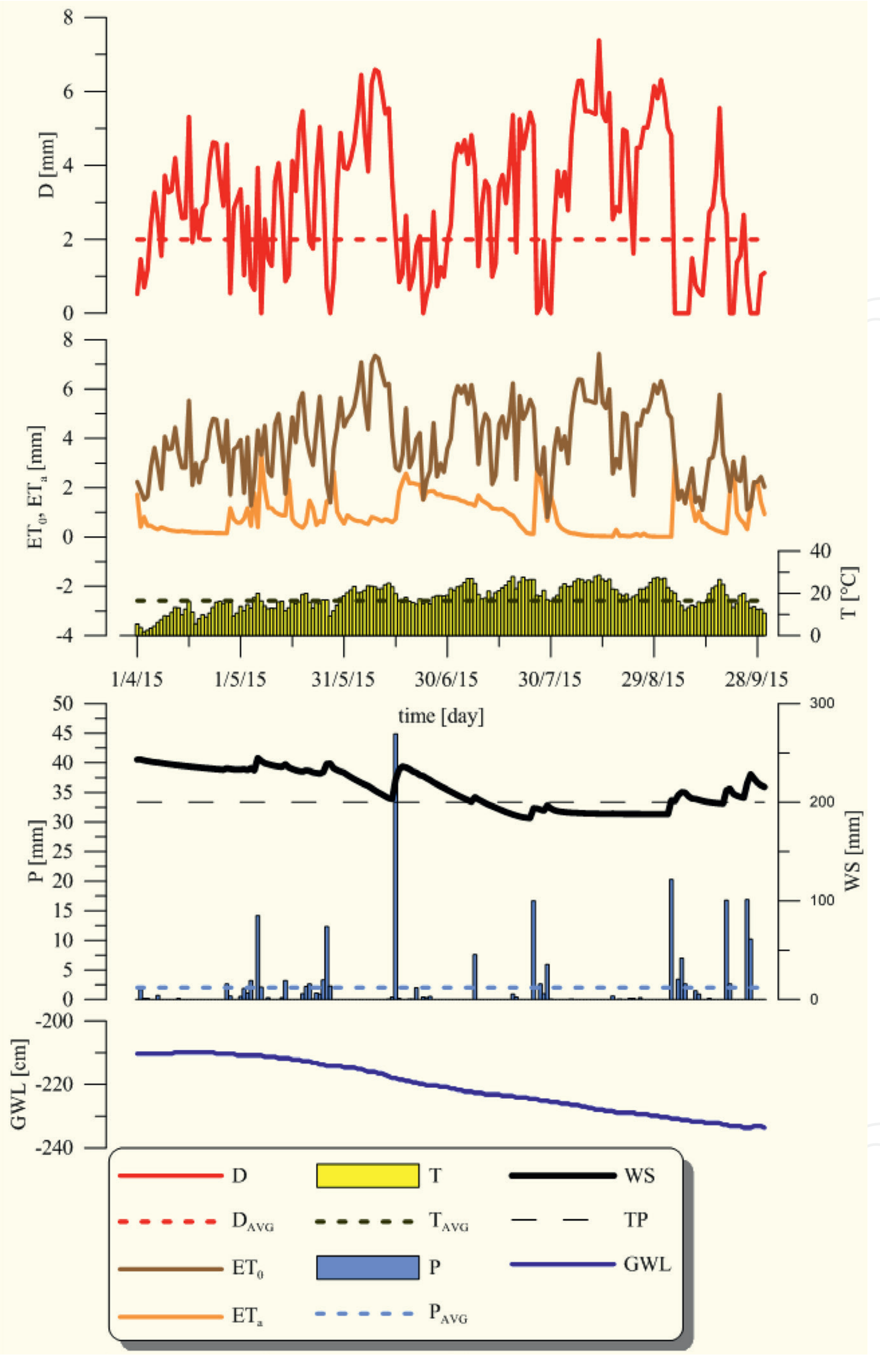

Figure 13.
Evapotranspiration deficiency and water regime elements in the extremely dry year of 2015.

water transfer from GWL to the root zone ceases. Moisture conditions in the balanced layer of the root zone depend solely on rainfall and evaporation. When there is the longer period with no rainfall, water supply towards the roots stops. The upper soil horizons and subsequently the whole root zone get into the state of drought. In **Figure 12** the examined years are ordered by mean soil water storage to the depth of 1 m during the growing season.

The scheme shows that the driest year in terms of soil water storage during a growing season was the year 2015. In consequence, water regime elements in 2015 were analysed. The results of the analysis were calculated with 1-day step and they are shown in **Figure 13**. Evaporation deficiency 'D' is 257% of the long-term mean (1971–2015). ET_0 is 134% and ET_a is 49% of the corresponding long-term mean. The mean temperature is relatively stable, 110% of the corresponding long-term mean. Rainfall 'P' formed 61% of the corresponding long-term mean and water storage in soil to the depth of 1 m 'WS' were 77% of the corresponding long-term mean. The results shown in **Figure 13** indicate that in the other half of the growing season soil water storage dropped under the point of decreased availability.

This corresponds to the fact that the value of 'D' was high above the average. Groundwater continuously drops during the whole growing season. **Figure 13** also shows the development and correlation between ET_0, ET_a and D.

4. Conclusions

Precipitation amount and temporal distribution of the rainfall is important for water refilling of the environment for balanced periods. Drying of soil profile occurs during long rainless periods. Meteorological drought and subsequently soil drought occurs in the case of the sufficiently long rainless period. Therefore it is necessary to know size and statistical characteristics of rainless periods (RLP). The aim of the contribution is to identify important rainless periods, quantify temporal lengths, probability characteristics and trends of RLP. Climatic station of Milhostov (N 48°39,786′; E 21°43,298′) was chosen for selection of statistically important rainless periods. Station represents wider area of lowland. Daily precipitation amounts of the 1961–2015 period was examined for the station. 20,080 daily precipitation amounts (including zero) were analysed for the period. Length of RLP was identified in two ways. Periods with zero daily precipitation amounts were considered in first selection (s0). Daily precipitation amounts lower than 2 mm were considered as zero in second selection (s2). The absolutely longest continuous period without rainfall for s0 selection (year, VP) had 35 days and occurred between 25.9.1962 and 29.10.1962. Maximal continuous rainless event extends to 53 days in case of s2 selection for the vegetal period. This event occurred in time interval 19.7.1967–9.9.1967. Number of rainy and rainless days is for individual years and their vegetal periods balanced in the long term view. Only duration of rainless events of non-vegetal periods changes in examined periods. Growth of time length of rainless days duration was identified in non-vegetal half-year.

The study analysed the development of ET_0, ET_a, D, WS, P, GWL location and T during the growing seasons during the years 1970–2015 on the basis of the measured data and the data gained via numerical simulation. The interaction processes in the root zone of a soil profile during the creation of soil water regime were quantified. The quantification is crucial for understanding the processes occurring during drought creation, duration and termination. It has been demonstrated that soil water storage depends heavily on evaporation, i.e. actual evapotranspiration ET_a. Subsequently, actual evapotranspiration influences on evapotranspiration deficiency 'D' and on the location of GWL. For that reason, evapotranspiration deficiency 'D' can be considered an indicator of the drying of a soil profile. Drying starts when water inflow towards plant roots is reduced. During the state of evapotranspiration deficiency, groundwater supplies the root zone of a soil profile with water. When there is the long period with no rainfall, water transfer from GWL towards plant roots ceases. Moisture conditions in the balanced layer of the root zone depend solely on rainfall and evaporation. The processes are demonstrated on the driest growing season of 2015. From the point of view of soil water storage to the depth of 1 m this season was absolutely driest growing season in the examined period from 1970 to 2015.

Acknowledgements

This work was created thanks to financial support of VEGA project 2/0062/16.

Author details

Milan Gomboš*, Branislav Kandra, Andrej Tall and Dana Pavelková
Institute of Hydrology, Slovak Academy of Sciences, Bratislava, Slovak Republic

*Address all correspondence to: gombos@uh.savba

References

[1] Van Genuchten M. A closed-form equation for predicting the hydraulic conductivity of unsaturated soils. In Soil Science Society of America Journal. 1980;**48**:892-898

[2] Majerčák J, Novák V. Simulation of the soil-water dynamics in the root zone during the vegetation period. I. The mathematical model. Vodohosp. Čas. 1992;**40**(3):299-315

[3] Novák V, Majerčák J. Simulation of the soil-water dynamics in the root zone during the vegetation period. II. The course of state variables of soil water below the maize canopy. Vodohosp. Čas. 1992;**40**(4):380-397

[4] Majerčák J, Novák V. GLOBAL, one dimensional variable saturated flow model, including root water uptake, evapotranspiration structure, corn yield, interception of precipitations and winter regime calculation. In Research Report, Bratislava, Institute of Hydrology, Slovak Academy of Sciences. 1994, 75 pp

[5] Šimůnek J, Huang K, Šejna M, Van Genuchten Th M, Majerčák J, Novák V, Šútor J. The HYDRUS - ET Software Package for Simulating the One - Dimensional Movement of Water, Heat and Multiple Solutes in Variably - Saturated Media. Version 1.1.1997, Institute of Hydrology S.A.S. Bratislava - U.S. Salinity Laboratory, Riverside, 1997, 184 pp

[6] Novák V, Šútor J, Majerčák J, Šimůnek J, Van Genuchten M Th. Modeling of Water and Solute Movement in the Unsaturated Zone of the Žitný Ostrov Region, Institute of Hydrology S.A.S. Bratislava, 1998 73 p

[7] Šoltész A, Baroková D. Analysis, prognosis and design of control measures of Ground water level regime using numerical modelling, Podzemná voda, XII, SAH, Bratislava 2006;č.2:113-123

[8] Šoltész A, Baroková D. Impact of landscape and water management in Slovak part of the Medzibodrožie region on groundwater level regime. In Journal of Landscape Management. 2011;**2**(2):41-45

[9] Červeňanská M, Janík A, Šoltész A, Baroková D, Gramblička M. Determination of input data for utilization of drainage channel systems on improvement of water regime in wetland systems. In Acta Hydrologica Slovaca. 2016;**17**(2):133-139

[10] Estokova A, Balintova M. 2018. Advances in Environmental Engineering. In ENVIRONMENTS. ISSN 2076-3298. 2018:**5**(5)

[11] Hlaváčiková H, Novák V, Kostka, Z, Danko M, Hlavčo J. The influence of stony soil properties on water dynamics modeled by the HYDRUS model. In Journal of Hydrology and Hydromechanics, 2018;**66**(2):181-188

[12] Igaz D, Šimanský V, Horák J, Kondrlová E, Domanová J, Rodný M, Buchkina N. Can a single dose of biochar affect selected soil physical and chemical characteristics. In Journal of Hydrology and Hydromechanics, 2018;**66**(4):421-428. ISSN 0042-790X